Biocatalysis and Agricultural Biotechnology 22 (2019) 101369

Contents lists available at ScienceDirect

Biocatalysis and Agricultural Biotechnology

journal homepage: http://www.elsevier.com/locate/bab

Upgrading the electrochemical performance of graphene oxide-blended sulfonated polyetheretherketone composite polymer electrolyte membrane for microbial fuel cell application

Mehri Shabani [a], Habibollah Younesi [a,*], Ahmad Rahimpour [b], Mostafa Rahimnejad [c]

[a] Department of Environmental Science, Faculty of Natural Resources, Tarbiat Modares University, Tehran, Iran
[b] Department of Chemical Engineering, Babol Noshirvani University of Technology, Shariati Ave., Babol, Iran
[c] Biotechnology Research Lab., Faculty of Chemical Engineering, Babol Noshirvani University of Technology, Babol, Iran

ARTICLE INFO

Keywords:
COD removal
Coulombic efficiency
Oxygen diffusion
Power density
Proton conductivity
SPEEK/GO composite membrane

ABSTRACT

In the present study, composite polymer electrolyte membranes were synthesized by the incorporation of graphene oxide (GO) in sulfonated polyetheretherketone (SPEEK) for simultaneous wastewater treatment and electricity generation. A variety of techniques were applied to characterize the chemical, crystal and morphological structure of the as-synthesized membranes. In addition, the water uptake, mass transfer, and oxygen diffusion coefficients, proton conductivity, ion exchange capacity, internal resistance, power density, coulombic efficiency and COD removal of the MFC system applied with SPEEK, SPEEK/GO composite membranes were studied and compared with the commercial Nafion117. The incorporation of various GO contents caused a decrease in oxygen diffusion and mass transfer coefficients of 7.45×10^{-6} cm^2 s^{-1} and 0.00048 cm s^{-1}, respectively. This was also shown that the SPEEK/GO3 membrane with proton conductivity 2.88 mS cm^{-1}, power density 53.12 mW m^{-2}, voltage 883 mV, and CE 3.74% showed higher performance compared to Nafion 117 membrane as a separator in MFC. Furthermore, the MFC with SPEEK/GO3 membrane gave slightly higher COD removal (88.7%) than that of MFC incorporating the Nafion 117 membrane (81.9%). The ion exchange capacity (IEC) and WU of as-prepared membranes were found to vary from 1 to 2.21 meq g^{-1} and from 44.31 to 67.85%, respectively. The results obtained were revealed that the MFC assembled SPEEK/GO3 composite membrane is demonstrated significant improvement in cell performance compared with commercial Nafion 117 membrane that qualifies it to be a promising candidate as a proton exchange membrane in the lab-scale microbial fuel cells.

1. Introduction

There is strong concern over the discharge of water used in the manufacturing process to wastewater streams and entering the rivers and estuaries (Kumar et al., 2019). To avoid the adverse impacts of wastewater on the environment and the aquatic ecosystem, it needs to be treated to meet certain discharge standards (Kumar and Bishnoi, 2017). Organic substrate present in various wastewater is a great potential to be applied for bioenergy harvesting, which brings the chance of wastewater treatment simultaneously. Many Aerobic and anaerobic treating methods have been used to treat wastewater (Hernández-Flores et al., 2016). Since aerobic treatment methods such as activated sludge need constant energy supply and also additional steps of sludge management. Concerns over the discharge of industrial polluted water into water bodies cause increasing attention to novel biologically treatment of wastewater to meet the standards of discharge. Among different anaerobically treatment methods, microbial fuel cells (MFCs) are a promising technology to treat the wastewater simultaneously with saving energy. MFC, as a bioelectrochemical hybrid system, is a topic of focus because of their anaerobic process of treatment and at the same time for energy saving, reduced sludge, nutrients recovery and their positive energy production as called bioelectricity harvesting (Rahimnejad et al., 2020; Sun et al., 2009). An MFC relies on electrochemically active bacteria as a biocatalyst that directly consumes the organic load of wastewater and produces electricity (Zhang et al., 2019). In an MFC system, the electrons produced by degrading organic wastes transfer to the electrode by means of active biofilms and pass to the cathode through an external circuit, which connects two chambers, for oxygen

* Corresponding author.
E-mail address: hunesi@modares.ac.ir (H. Younesi).

https://doi.org/10.1016/j.bcab.2019.101369
Received 30 June 2019; Received in revised form 16 September 2019; Accepted 30 September 2019
Available online 1 October 2019
1878-8181/

reduction reaction to produce H_2O. Therefore, the suitable passage of ions should be provided in order to achieve charge balance and for this means, ion exchange membranes separate the two chambers. In many cases, convention commercial separators such as Nafion have been applied in both conventional fuel cells (FC) and MFCs, which apart from their many similarities, their big difference is the use of microorganisms in the anode (Koók et al., 2019a). Nafion has been the only choice in MFCs for long. In recent years, there has been a serious effort to develop a low-cost polymer electrolyte membrane to replace Nafion due to some of its limitations including substrate loss, oxygen leakage from cathode to anode, cation transport rather than protons, and biofouling (Angioni et al., 2016; Chae et al., 2008). In most studies, applied membranes in the systems are chemically-synthetized from polymers (Bakonyi et al., 2018; Koók et al., 2019b). Regardless of the initial materials, the membranes applied in MFCs should meet some important properties such as mass transfer to the electrode, low resistance, high proton conductivity, sustainability for a long period, selectivity, cost, and oxygen permeability (Mauritz and Moore, 2004). Therefore, the applied separators play a key role among the parameters affecting the efficiency of two-chamber MFCs.

In general, various types of cation exchange membranes (CEMs) and modified polymers have been used such as sulfonated polyetheretherketone (SPEEK) (Chae et al., 2014; Seetharaman et al., 2013), polyethersulfone (PES) (Daud et al., 2011; Lim et al., 2012; Rahimnejad et al., 2012; Zinadini et al., 2017), polysulfone (PS) and sulfonated (SPS) polysulfone (Bunlengsuwan et al., 2017; Ghasemi et al., 2016) and polybenzimidazole (PBI) (Hwang et al., 2014; Mamlouk and Scott, 2011). They all are categorized as non-fluorinated membranes which are low-cost and cause little pollution to environmental (Zhao, 2018). These types of polymers contain aromatic structures and the benzene ring in the backbone or in the pendant groups attached to the membrane polymeric backbone (Genovese and Villante, 2014). However, CEMs, which refer to as proton exchange membranes (PEMs), are penetrable to the protons, because of their low internal resistance and high conductivity, and instantaneously avoid channeling oxygen substrate from the cathode to anode chambers. The efforts have been made on modifying the polymeric membranes either by blending two polymers, sulfonation of aromatic polymers or additional of nanoparticles to improve their efficiency. The sulfonation of the aromatic polymer is one of the efficient and easiest methods that improve proton conductivity, hydrophilicity and solubility of the membranes (Zinadini et al., 2017). Recent investigation was shown that the addition of silicon dioxide (SiO_2) to sulfonated graphene oxide (GO) blended with poly(vinylidene fluoride) grafted sodium styrene sulfonate (PVDF-g-PSSA) caused improvements in the proton conductivity and anti-fouling of PEM in MFCs compared with Nafion membrane (Xu et al., 2019). Furthermore, some studies focused on blending polymers with various contents of polymers for the aim of examining the possible as PEMs (Daud et al., 2011; Lim et al., 2012; Tiwari et al., 2016; Yin et al., 2016). For example, a study was investigated polymer blend membrane of poly(amideimide) (PAI) and SPEEK, which resulted in proton conductivity and power density in MFC (Sowmya and Prabhu, 2018). The sulfonated PEEK polymer provides the advantages of great features and excellent resistance performance, excellent thermal and chemical stability, hydrophilicity, easy preparation, high mechanical strength, lower cost and modest proton conductivity over the existing proton conducting polymers (Zaidi, 2005). However, a higher efficient sulfonated polymer provides a higher ion exchange capacity (IEC) and increases the proton conductivity due to the formation of water nanochannels between the hydrophobic aromatic and the hydrophilic sulfonic acid groups (Kamaroddin et al., 2019). On the other hand, considering the MFC technology scaling up, many of these novel membranes are not suitable compared to Nafion (Lim et al., 2012), so studies should be continued to recommend a suitable membrane to replace the Nafion. Graphene is a hydrophilic compound with a pseudo-neodymium structure and exhibits high electrical conductivity due to a large number of free electrons (Cao et al., 2018; Changkhamchom and Sirivat, 2010). The incorporation of oxygen-containing functional groups on both sides of the plate and the edges of graphene oxide gives a water-rich property, which results in excellent dissolution in organic solvents and helps to uniformly distribute the material in the membrane solution. In addition, the sp^2 carbon layer in the hydrophobic region of this compound can help increase the mechanical strength of the membrane due to strong covalent bonding (Eck and Krueger, 2013).

The aim of the present study was to improve the efficiency, proton conductivity, and hydrophilicity of polyetheretherketone (PEEK). Thereon, sulfonated polyetheretherketone (SPEEK) is incorporated into nanosize graphene oxide (GO) by dry phase inversion method. The effects of different ratios of nanosheets and also the ratio of polymer concentration were investigated for the first time in the MFC system. Finally, the comparison of as-synthesized membranes was conducted with commercial Nafion117 in terms of water uptake, proton conductivity, oxygen diffusion, voltage, power density, coulombic efficiency, and COD removal efficiency.

2. Materials and method

2.1. Preparation of sulfonated polyetheretherketone

Sulfonated polyetheretherketone (SPEEK) was prepared using 98% concentrated sulfuric acid (H_2SO_4). Briefly, 5 g of polyetheretherketone (PEEK) (Goodfellow Cambridge Limited, UK) powder was dried for 12 h at 100 °C and was slowly added into 100 ml of the concentrated H_2SO_4 (Merck, Germany) with continuous stirring for 4 h at room temperature. After aging at 50 °C for 2 h, the polymer solution was gradually precipitated in ice water under strong mechanical stirring. Finally, the precipitated polymer was filtered and washed several times with deionized water (DI) till achieving neutral pH and then vacuum dried at 60 °C for 12 h followed by 90 °C for another 12 h (Chae et al., 2014). At this step, the color of the dried sulfonated polymers turned to light brown. The existence of sulfonic acid groups in the SPEEK polymer was identified using the traditional titration method (Zhao et al., 2018).

2.2. Preparation of graphene oxide

Graphene oxide (GO) was prepared based on the modified Hammer method (Hummers and Offeman, 1958; Lv et al., 2013). Typically, 3 g of graphite powder (Gr) and 2 g of sodium nitrate ($NaNO_3$) were added into a 500-ml beaker containing 60 ml H_2SO_4 and the beaker was placed in an ice bath. After 30 min stirring, 10 g potassium permanganate ($KMnO_4$) was gradually added to the above mixture. At this step, the color of the mixture was turned to dark green. After the complete dissolution, the beaker was then left to stir at room temperature for 3 h and increased the temperature at 35 °C and stirring for 5 h followed by diluting slowly with 120 ml of DI water in an ice bath and stirred for another 12 h at 70 °C. The temperature of the dark brownish mixture was reduced to 45 °C. Subsequently, 35 ml hydrogen peroxide (H_2O_2) was slowly added into the mixture followed by diluting with 50 ml of DI water and stirring for 2 h. At this step, the color of the mixture was turned to dark yellow. The mixture was then centrifuged (universal 320R) at 5000 rpm for 30 min and the supernatant was discarded to leave only the precipitate. The precipitation was then washed with 5% hydrochloric acid (HCl) followed by DI water to obtain the neutral pH. The product was then dried using a freeze-drier (Operon Co., Ltd.). The GO mixture was obtained by dispersing a specific amount of graphite oxide (GrO) in DI water and ultrasonicated (Elma, 120H) for 60 min at 60 kHz and 750 W until a homogeneous mixture was obtained and centrifuged at 5000 rpm for 30 min and dried in air at 70 °C for 24 h to obtain the final product. All chemicals were purchased from Merck (Merck KGaA, Darmstadt, Germany) and used without further purification.

2.3. Synthesis of SPEEK and SPEEK/GO composite membranes

SPEEK and SPEEK/GO membranes were fabricated by the dry-phase inversion method. Briefly, two different ratios of SPEEK membrane casting solution (15 and 20%) were prepared by dissolving the defined amount of sulfonated polymer in dimethylacetamide (DMAc) (Merck, Germany) and stirring for 24 h at 600 rpm to obtain the homogeneous solution. For the preparation of SPEEK/GO membrane solution, certain amounts of GO were slowly added into the same amount solvent and then sonicated for 30 min followed by stirring for 3 h. Then, SPEEK was added to the solution followed by continual stirring for another 24 h to obtain 1, 3 and 5 wt% SPEEK/GO solution. The solution was then left to stand for at least a 24-h period until trapped dissolved air bubbles were removed. SPEEK and SPEEK/GO clear homogeneous solution was cast onto flat glass using casting knife with 180 μm thickness, dried at room temperature for 3 h followed by oven heating at 70 °C for 24 h and annealing at 100 °C for 8 h. After the flat sheet membrane cooled at ambient temperature, it was immersed in DI water and peeled from the glass plate. Finally, the membrane was cut into ring shape around 5 cm diameter, activated by 1 M H_2SO_4 for 12 h, and stored in DI water for further use (Leong et al., 2015). Table 1 shows the chemical composition of as-prepared membranes using various GO and SPEEK ratios.

2.4. Degree of sulfonation and ion exchange capacity (IEC)

IEC is a very important factor in MFCs defined as the amount of ion exchange of the membrane. The IEC of the SPEEK, which is referring to its hydrogen ion of sulfonic acid groups, was determined using the titration method. About 0.5 g of SPEEK-H was immersed into 0.01 M sodium hydroxide (NaOH) solution (200 ml) for three days, which was found to be sufficient to convert SPEEK-H into SPEEK-Na (SPEEK-Na is a copolymer, consisting of PEEK-SO_3Na unit and PEEK unit). Dilute solution of H_2SO_4 (0.03 M) was employed to back-titrate the NaOH solution, which has been partially neutralized by the SPEEK-H sample. Phenolphthalein was adopted as the universal indicator to help determine the neutral point. By measuring the number of H_2SO_4 consumed in the titration, the molar quantity of the sulfonic acid groups (-SO_3H) contained in the SPEEK-H sample can be determined according to the following equation (Othman et al., 2007):

$$N_{SPEEK-Na} = (M \times V)_{NaOH} - 2(M \times V)_{sulfuric\ acid} \quad (1)$$

where, M and V are the molar concentration and the volume of the solutions, respectively. The IEC can then be estimated by using the following equation:

$$IEC = \frac{N_{SPEEK-H}}{W_{Sample}} \times 1000 \quad \left(\frac{meq}{g}\right) \quad (2)$$

where $W_{example}$ is the weight of the SPEEK-Na sample and $N_{SPEEK\text{-}H} = N_{SPEEK\text{-}Na}$. The degree of sulfonation (DS) can be calculated from IEC by using the following equation:

$$DS = \frac{288\ \ (IEC)}{1000 - 102\ \ (IEC)} \quad (3)$$

Table 1
Chemical compositions of prepared separators used in MFCs.

Composition	SPEEK15	SPEEK20	SPEEK/GO1	SPEEK/GO3	SPEEK/GO5
SPEEK	15%	20%	15%	15%	15%
GO	0	0	1%	3%	5%
DMAc	85%	80%	84%	82%	80%

2.5. Water uptake (WU), oxygen diffusion and proton conductivity

Water uptake (WU) for a membrane is defined by the amount of water sorbed superficially or hydrogen-bonding bonded to the interstitial sites and surface (Seo et al., 2013). In order to maintain ion conductivity and mechanical strength, there is a threshold amount of water presented in the membrane matrix. An excessive percent of water makes the membrane losing the mechanical properties, while its storage causes brittle in the membrane (Pupkevich et al., 2007). Membrane samples with a surface area of 5 cm^2 were dried in a vacuum oven at 80 °C for 24 h until they remain a constant weight (W_{dry}). Then, the dried membranes were soaked in DI water for 1 day at room temperature. The water on the surface was carefully eliminated with tissue paper and then the samples were weighed again (W_{wet}). The water absorption of the membrane is calculated by the following equation (Duan et al., 2013; Zawodzinski et al., 1993):

$$Water\ uptake = \frac{W_{wet} - W_{dry}}{W_{dry}} \times 100 \quad (4)$$

where W_{dry} and W_{wet} are the weight of the membrane samples in the dry situation and the weight of the membrane in a wet state after the soaking into DI water, respectively.

The presence of dissolved oxygen (DO) in the anode chamber causes the reduction in coulombic efficiency as it plays the role of electron acceptor and results in loss of electron donors, and also inhibit the growth of obligate anaerobes. Therefore, the as-synthesized membranes must be observed and analyzed in terms of oxygen transfer. To do this, a dual-chamber MFC was set up. The two assembled chambers were filled up with DI water. The anode chamber was purged with N_2 gas to reach the DO level lower than 0.5 mg l^{-1}. While the cathode was continuously aerated, the DO changes of the anode were taken at 1-h intervals for the duration of 9 h. The DO concentration was measured using a DO probe (WTW Multi 3630 IDS, UK). The oxygen mass transfer coefficient (k_0) (cm s^{-1}) and oxygen diffusion coefficient (D_0) (cm^2 s^{-1}) were determined using the following equations:

$$k_0 = \frac{V}{At} ln \frac{C_0 - C}{C_0} \quad (5)$$

$$D_0 = k_0 L \quad (6)$$

where, V is the anode volume (cm^3), A the surface area of membranes (cm^2), C_o is DO concentration (mg l^{-1}) in the cathode chamber which is saturated, C the DO concentration (mg l^{-1}) in the anode at time t (s) and L the membrane thickness (cm).

In the present study, the resistance of the membranes was measured using a membrane conductivity test system (MCTS-A1, Iran) over the resistance ranging from 30 mΩ to 30 kΩ at a relative humidity of 100% and at room temperature. The composite membranes were first pretreated with 1 M H_2SO_4 for 12 h followed by maintaining at DI water for 24 h before analysis. The proton conductivity of the membrane was computed from the resistance data as follows:

$$\sigma = \frac{L}{RA} \quad (7)$$

where, σ is the proton conductivity of membrane (S cm^{-1}), L the membrane thickness (cm), R the ohmic resistance of membrane (Ω), and A is the membrane surface area (cm^2).

2.6. Characterization techniques

The chemical structure of pristine Gr and as-synthesized GrO and nanosheet GO and the as-synthesized membrane was analyzed with the Fourier transform infrared spectroscopy (Thermo Nicolet Avatar FTIR 380, USA) in the range between 400 and 4000 cm^{-1}. A Raman spectrum was were recorded with a micro spectrometer (Takram P50C0R10)

between 400 and 4000 cm^{-1}. The crystalline structure was recorded by an X-ray diffractometer (XRD, Philips, PW1730) operated at a voltage of 40 kV and at room temperature employing a scanning rate of 0.02 degrees per second with CuKα radiation (λ = 1.54056 Å) in a 2θ range of 5° to 80°. The interlayer distance for the as-synthesized sample is computed on the basis of the Bragg's law:

$$d = \frac{\lambda}{2sin\theta} \quad (8)$$

Transmission electron microscopy (TEM) images were obtained by using a Philips CM120, 120 kV to study the morphological features of GO. The cross-sectional images of the as-prepared SPEEK and SPEEK/GO composite membrane with different GO content were characterized by the field emission scanning electron microscopy (FESEM- TESCAN, MIRA III). The membrane samples were fractured in the liquid nitrogen followed by gold sputter coating prior visualization under the FESEM.

2.7. COD removal and coulombic efficiency (CE)

Many parameters, including microbial growth, aerobic and anaerobic growth by electron acceptors in the bed and electrode surface in the batch mode operation, may affect the rate of COD removal in MFCs (Tommasi and Lombardelli, 2017). Whereas, the condition of microbial communities depends on different operating conditions that may affect the COD removal. The COD removal efficiency in the anode chamber was calculated as follows:

$$COD\ removal = \frac{COD_o - COD_f}{COD_o} \quad (9)$$

In general, many factors such as aerobic respiration of the cathode biofilm, the electron consumption by methanogenesis and oxygen crossover limit the coulombic efficiency (Heilmann and Logan, 2006). In order to measure the amount of COD removal achieved by the end of a cycle, it is satisfactory to report the coulombic efficiency (CE) (Kim et al., 2010).

This parameter is presented as the ratio of total coulombs that actually transferred from the substrate to the anode (Rabaey et al., 2005). The obtained total coulombs was determined by integrating the current over time so that the coulombic efficiency for an MFC run in the batch mode, evaluated over a period of time t, was calculated as follows (Logan and Verstraete, 2017):

$$CE = \frac{M \int_0^t I\, dt}{Fbv_{An}\Delta COD} \quad (10)$$

where M is the oxygen molecular weight is (32 g/mol), F the Faraday's constant (96485 C/mol), b the number of electrons exchanged per mole of oxygen (4 mol e^-/mol O_2), v_{An} the volume of liquid in the anode chamber (l), and ΔCOD the change in COD concentration over time t (g/l).

2.8. Power density

It is a measurement of the voltage and the power as a function of current density (polarization curve) in order to characterize the performance of an MFC under constant operating conditions. The maximum power density is achievable by experimental manipulation of circuit resistance which results in the polarization curve (Lee et al., 2008). While obtaining the polarization curve, a range of 0.5–8 kohm resistance has been applied to the cell. The power density was measured by the following equation:

$$\text{Power density } \left(mW/m^2\right) = \frac{\text{Cell voltage (v)} \times \text{Electrical current (A)}}{\text{Anode surface area } (m^2)} \quad (11)$$

2.9. MFC set-up

Generally, an MFC consists of an anaerobic chamber called anode, and the aerobic cathode (sometimes biocathode) that may or may not be separated by a proton selective membrane (Kumar et al., 2019). In the present study, a dual-chamber MFC system with a working volume of 800 ml in each chamber was fabricated from Plexiglass material. The dimension of each chamber was 130 (length), 110 (width) and 60 (depth) mm, with an approximate volume of 860 ml. The performance of lab-scale MFC under different batch-mode conditions was conducted in terms of COD removal percentage, power production, and coulombic efficiency. The performance of membranes (Nafion 117, Sigma-Aldrich and the as-synthesized membrane) that fixed between two chambers were tested as electrolytes separator. Prior to use in the MFC system, the membranes were treated by boiling in a 30% hydrogen peroxide (H_2O_2) solution, 0.5 M sulfuric acid (H_2SO_4) solution and rinsed in DI water for about 1 h. The inoculums in the anode chamber were made up of industrial wastewater and anaerobic mixed bacteria sludge; taken from a sewage treatment plant (Chamestan Industrial Park). The cathode compartment has been applied without any catholyte chemical control. The average value from the four replicate analyses with a relative standard deviation (SD) and range values of the wastewater characteristics are provided in Table 2. The initial COD of all systems was around 2000 mg l^{-1}. The nitrogen gas was purged to the anolyte for 10 min to keep the anode chamber in an anaerobic condition at the start of each cycle. The anaerobic condition of the anode chamber was daily checked during the 5 days run. Air was continuously purged into the cathode chamber using an air pump to supply oxygen for the oxygen reduction reaction at the cathode. The carbon clothes with the size of (3×4 cm) were used as electrode materials after the activation process. The voltage values were determined without any mediator compounds. A data logger was connected to the MFC to record the voltage output of the MFC system at intervals of 15 min. The MFC system was left to operate for 5 days to achieve the stable voltage and power.

3. Results and discussion

3.1. GO characterization

Fig. 1 shows the FTIR spectra of pristine Gr and as-synthesized GrO and GO. As it is expected, the pristine Gr spectrum exhibits very weak peaks, while the spectra of both oxidized products of GrO and GO show several strong characteristic peaks of oxygen-containing functional groups. In the pristine Gr spectrum, the weak peaks agreed to = CH_2 asymmetric and symmetric stretching at 2935 and 2853 cm^{-1} and peaks detected at 3750 and 660 cm^{-1} are expected to be for the stretching and bending vibrations of the C–H bond, respectively (Hayyan et al., 2015). In the spectra of GrO and GO, the peaks located at 1020 and 1041 cm^{-1} are ascribed to a stretching vibration from the C–O–C bonds of alkoxy group and peaks appeared at 995 and 982 cm^{-1} are corresponded to C–H bending vibration in methylene and methyl groups, respectively. In the spectrum of GrO, the band at a wavenumber of 1101 cm^{-1} may correspond to asymmetric C–O–C stretching vibrations of epoxide groups. In

Table 2
Measured characteristics of wastewater used in the anodic chamber.

Parameters	Average value ± SD[a]	Range value
pH	6.60 ± 0.42	6–6.9
Chemical oxygen demand (COD) (mgl^{-1})	1963.57 ± 135.60	1785–2190
Biological oxygen demand (BOD_5) (mgl^{-1})	896.14 ± 42.00	830–952
Nitrate-N (mgl^{-1})	70.88 ± 2.24	68.02–74.30
Phosphate-P (mgl^{-1})	9.02 ± 0.31	8.54–9.30
Total kejeldal nitrogen (TKN) (mgl^{-1})	19.32 ± 0.55	18.45–20.10
Total dissolved solids (TDS) (mgl^{-1})	992.86 ± 112.70	890–1226
Total suspended solids (TSS) (mgl^{-1})	2632.14 ± 426.00	2045–3112

[a] SD denotes the standard deviation of the measurements.

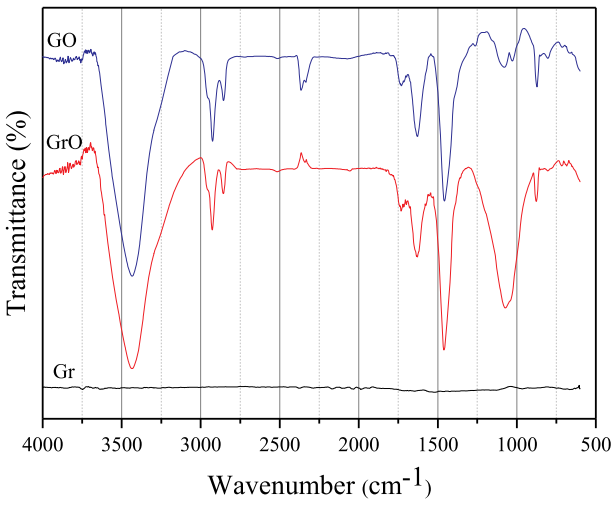

Fig. 1. FTIR spectra of graphite, graphite oxide and graphene oxide.

the spectrum of GO, the characteristic absorption band observed at 1216 cm^{-1} is attributed to C–OH stretching vibration of alcoholic groups (Kumar et al., 2014). A peak located at 1346 cm^{-1} is ascribed to C–O band of stretching vibration of the carboxyl functional group (Bykkam et al., 2013). In GrO and GO spectra, the peaks located at 1617, 1615 cm^{-1} are ascribed to the C═C stretching mode of sp^2 hybridized carbon structure (Alazmi et al., 2016). The stretching and bending vibration mode of –OH formed peaks at 3400 and 650 cm^{-1}, showing the evidence of hydroxyl functional groups decorated to the Gr and GO. The same results were achieved in a study done by (Amiri et al., 2016), confirming that the as-synthesized GO has a peak located at 1081 cm^{-1}, which was identified for the C–O bond. The peaks in the range of 1630 cm^{-1} to 1650 cm^{-1} show the C═C bond and The absorbed water in GO is shown by a broad peak at 2885 cm^{-1} to 3715 cm^{-1} (Dimiev and Tour, 2014). Finally, the presence of ample oxygen-containing functional groups in GO possesses an excellent hydrophobic nature, which plays a significant role in the hydrophilicity, dispersibility and compatibility behaviors in aqueous and organic solvent solutions (Feng and Guo, 2019). These results are in good agreement with those from earlier reports (Marcano et al., 2010; Rattana et al., 2012).

The XRD used to measure the average spacing between interlayers of atoms and determine the orientation of a single crystal or grain. Fig. 2 shows the XRD patterns of pristine Gr, GrO, and GO. XRD analysis shows an intense peak corresponding to the plane (002) of the highly organized interlayer structure of pristine Gr at $2\theta = 26.5°$ with an interlayer distance of 3.36 Å. A broad peak appeared at about 10.5° after oxidation of Gr flakes, corresponding to the interlayer distance of 3.34 Å, while a broad peak assigned to the crystal plane (001) of GO at $2\theta = 11.04$ with the interlayer spacing of 8.01 Å is observed after exfoliation of GrO flakes. The XRD pattern shows that the disappearance of the peak at 26° and the appearance of the peak at 10° confirmed the complete formation of GO after chemical oxidation and exfoliation (Wu et al., 2012). In addition, the interlayer distance for GO is significantly larger than pristine Gr and GrO due to the amorphization and incorporation of various oxygen-containing groups (Bhawal et al., 2016).

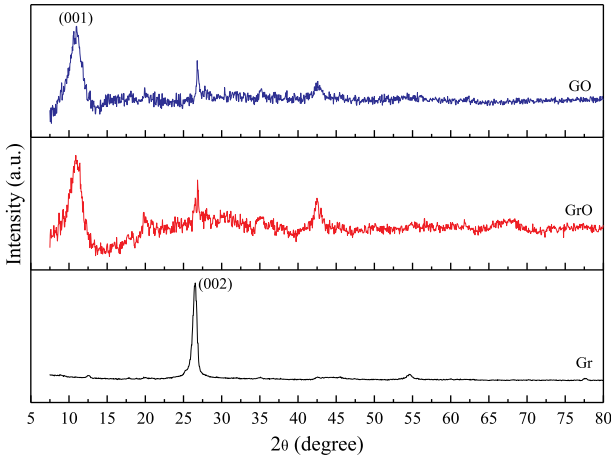

Fig. 2. XRD spectrum of Gr, GrO and GO.

Since Raman spectroscopy is useful for studying disorder and defects in the crystal structure, it is often employed to characterize Gr and its derivatives. The disorder is determined by the intensity ratio between the disorder-induced D band and the Raman allowed G band (I_D/I_G). Fig. 3 shows Raman spectra of the pristine Gr, as-prepared GrO and GO. According to the Raman results shown in Fig. 3, the high-intensity peaks are believed to be related to the conjugated π bonds and carbon-carbon double bonds. In the Raman spectrum of pristine Gr, a 2D band appeared at about 2900 cm^{-1} is corresponded to the overton of the D band. However, the typical Raman spectra of pristine Gr, GrO and GO are characterized by a G band located at about 1566 cm^{-1} and a D band observed at 1344 cm^{-1}. The increase of I_D/I_G from 0.45 of Gr to 1.36 of GO confirms the grafting of oxygen-containing functional groups to the graphitic planes. In functionalized graphene sheets, the higher intensity ratio of I_D/I_G indicates the higher disorder of π conjugated aromatic carbon-structure, demonstrating that the exfoliation and edge functionalization is initiated interlayer spacing by disruption of the graphitic carbon (Amiri et al., 2016). It was reported that an increase of the I_D/I_G ratio from 0.7 of Gr to 1.03 of GrO is a result of suitable edge oxidation and functionalization of graphitic carbon (Perumbilavil et al., 2015). The observation is inconsistent with FTIR and XRD results, which confirmed the presence of a high level of defects.

The morphological confirmation of truly synthesized GO is shown in Fig. 4. The TEM images result that a single layer of GO nanosheets and

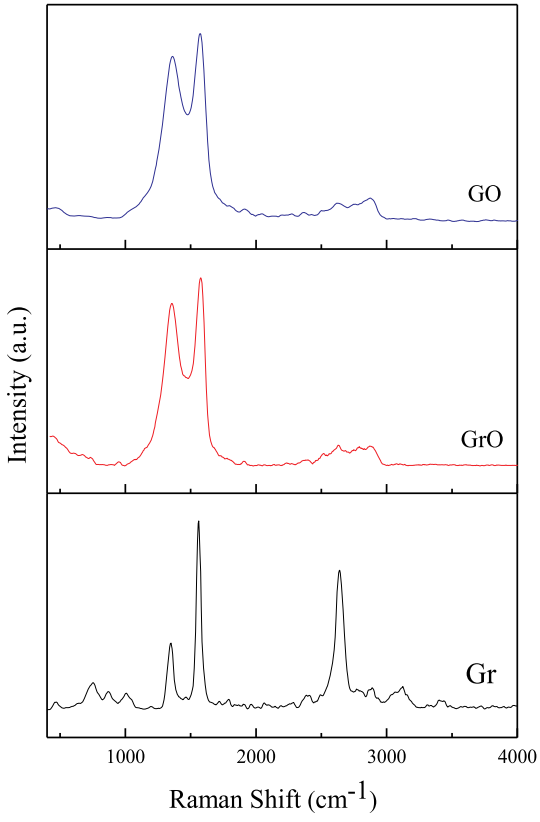

Fig. 3. Raman spectrum of pristine Gr, GrO and GO.

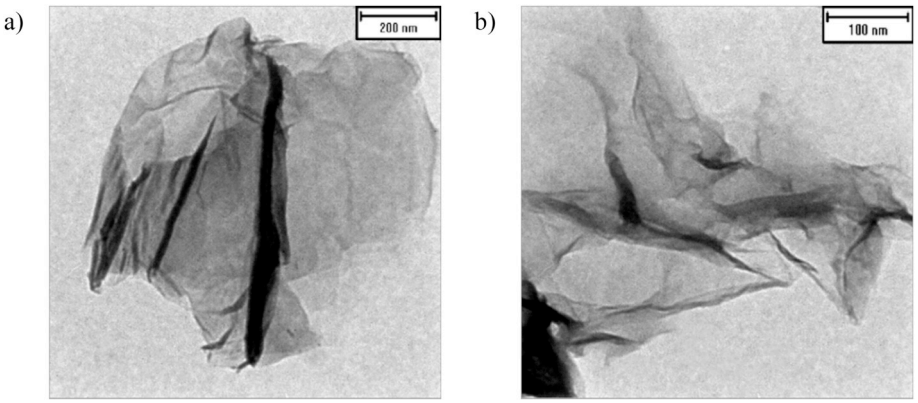

Fig. 4. The TEM images of GO.

folded edges are properly exfoliated from pristine Gr and it is consistent with literature reported morphology (Kumar et al., 2014; Leong et al., 2015; Lin et al., 2018). These figures show graphene flakes with high transparency, curved surface and without graphite crystal structure, confirmed that the wrinkle morphology created from the crumpling of graphite rather than stacking as evident by the sharp 2D bands in the Raman spectra.

3.2. Characterization of the composite membranes

In order to improve the proton conductivity of polymer electrolyte membranes, the hydrophilic region should be introduced to PEEK polymer, which can be achieved by introducing acid groups to both long and short side chains of polymer electrolytes simultaneously (Kumar et al., 2014). Herein, the sulfonated PEEK with sulfonic acid group loading was prepared and combined with GO nanosheets to synthesis nanocomposite membranes. Fig. 5 shows the FTIR spectra of fabricated SPEEK and SPEEK/GO membranes. The FTIR analyses revealed the presence of sulfonic acid groups (-SO_3H) in the polymers. A peak appeared at about 3424 cm^{-1} is corresponded to the stretching vibration of the O–H group and peaks located at 1265 cm^{-1} and 1089 cm^{-1} are ascribed with asymmetric and symmetric stretching vibrations of O═S═O in the sulfonic acid groups. In addition, a band at about 1037 cm^{-1} and 723 cm^{-1} due to the presence of S═O and S–O stretching vibration, respectively, were observed. For the SPEEK/GO membrane, the corresponding bands located at 1265 cm^{-1} and 1089 cm^{-1} are shifted to 1199 cm^{-1} and 1070 cm^{-1} because of the interactions between GO and SPEEK as a result of formation of hydrogen bonds between the –SO_3H groups and the polar oxygen-containing groups (hydroxyl and carboxyl groups) present in the GO sheets. The indicated trend of peak shifts is consistent with the reported values in other studies (Changkhamchom and Sirivat, 2010; Dai et al., 2014).

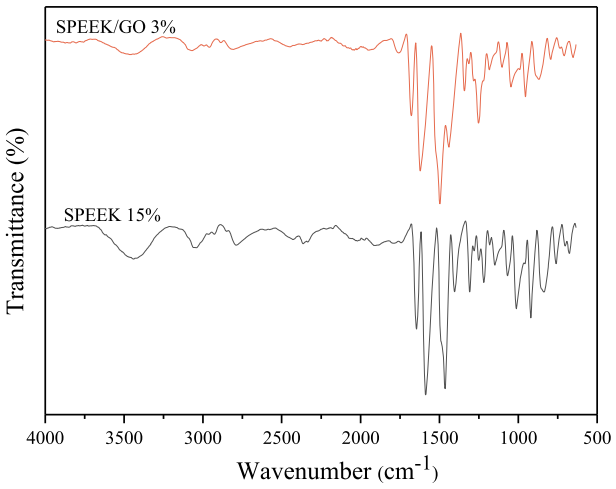

Fig. 5. FTIR spectra of fabricated membranes.

Fig. 6(a–e) presents FESEM imaging of cross-section of SPEEK and SPEEK/GO membranes. A major advantage of sulfonated polymer is that the suitable separators in MFCs are those which are nonporous to prevent oxygen and substrate crossover. From the FESEM images, we can see that our results confirm the nonporosity of all sample membranes. As shown in Fig. 6(c), (d), and (e), the GO nanosheets presented in the cross-section of composite membranes showed a homogenous distribution and affective interconnection between nanosheets and polymer matrix which increase membrane performance efficiency of a PEM in terms of power density. This was probably due to an interaction between the sulfonic acid groups of SPEEK and the oxygenated group of GO through hydrogen bonding. Our findings also confirm from previous results reported in the literature (Leong et al., 2015). In addition, the uniform distribution of incorporation of sulfonated GO into the SPEEK polymer matrix was confirmed. (Heo et al., 2013).

3.3. Physicochemical properties

The main goal of SPEEK-based electrolyte composite membranes is based on the compounds involving oxides, phosphates, sulfates, and water-containing systems present in the polymer structure through the Grotthuss mechanism, which postulates that protons undergo structural diffusion via the hydrogen bond network of water (Fischer et al., 2018). The results of water uptake (WU), ion exchange capacity (IEC), oxygen diffusion, and proton conductivity are presented in Table 3. The IEC estimated from the titration method was measured to be at 1.5 and 1.3 meq g^{-1} for bare SPEEK15 and SPEEK20, respectively, whereas IEC values of the SPEEK/GO1, SPEEK/GO3 and SPEEK/GO5 composite membranes were obtained to be 1.57, 2.21 and 1.93 meq g^{-1}, respectively. An increase in WU and IEC has been observed in SPEEK membranes after incorporation of GO due to its hydrophilic feature and a variety of oxygenated functional groups in its structure (Reyes-Rodriguez et al., 2017). As expected, membranes with the higher IEC showed an increase in water absorption, possibly due to their hydrophilicity and free volume property. This means that the repulsion of hydrophilic –SO_3H groups from the hydrophobic backbone of PEEK causes the formation of free volumes in the membrane for water molecules to be absorbed (Bykkam et al., 2013). As shown in Table 3, all the as-synthesized membranes obtain higher WU within a range from 55.00 to 67.85, than the commercial Nafion 117 membrane (44.31%). The highest WU value of 62.72% was achieved for SPEEK/GO3, while for bare SPEEK15 and SPEEK20 was obtained to be 58.2% and 55%, respectively. The reason for high WU in SPEEK membranes is related to the presence of sulfonic acid group (-SO_3H), which more water

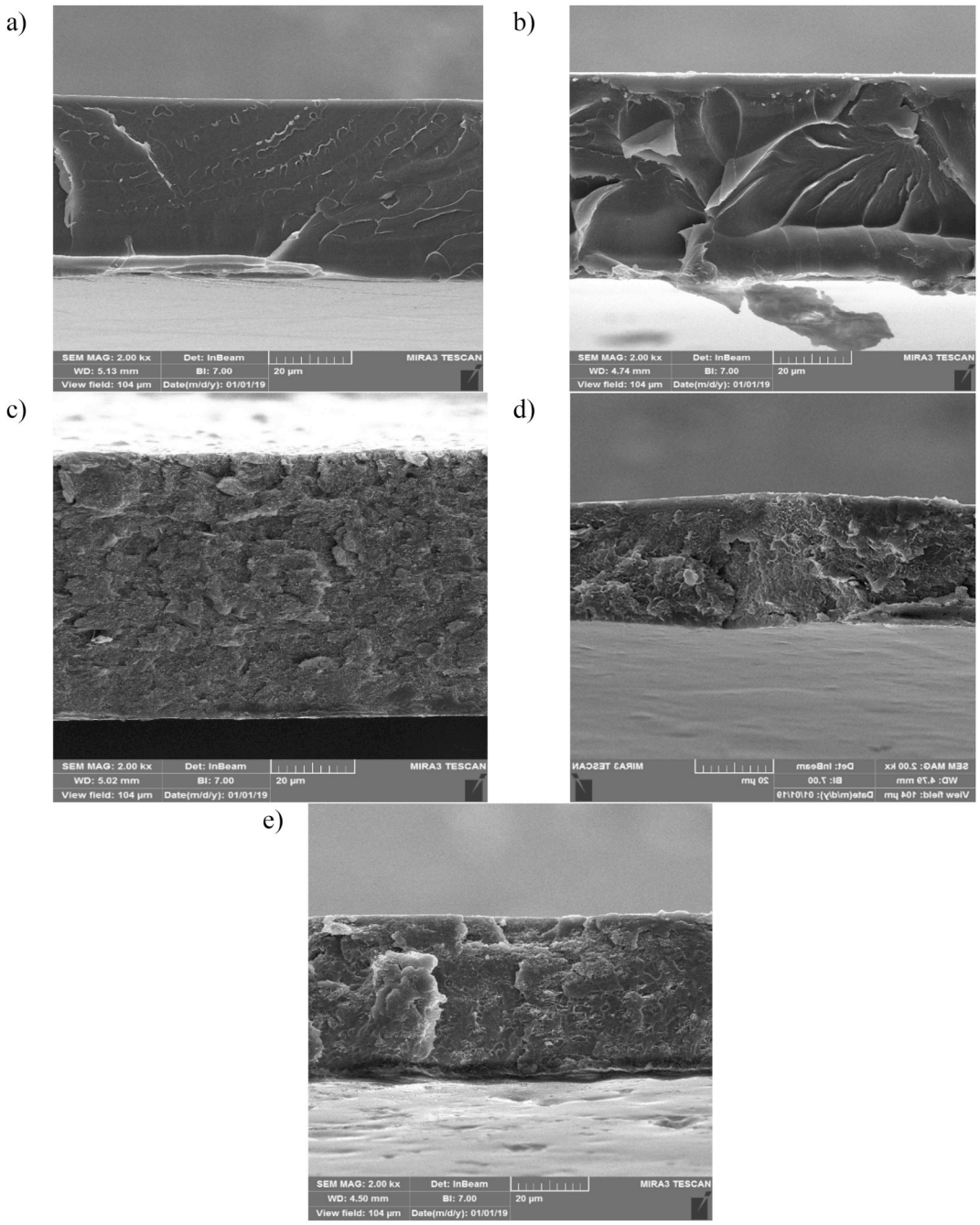

Fig. 6. FESEM images of cross-section for (a) SPEEK15, (b) SPEEK20, (c) SPEEK/GO1, (d) SPEEK/GO3 and (e) SPEEK/GO5.

electrolytes hold in the free volume of the membrane matrix (Wu et al., 2019). In addition, the high IEC of membrane increased with the degree of sulfonation (DS). In the present study, the degree of sulfonation SPEEK polymer was obtained to be around 60% based on the titration method. These results were in good agreement with the previous study (Leong et al., 2015).

As an attempt to synthesis a high-performance electrolyte membrane for the MFC system, WU directly affects the ability of membrane in proton conductivity. Consecutively, it should be noticed that large quantities of WU associated with the membrane swelling cause loss of its normal shape and typically form a membrane which tends to wrinkle upon drying at room temperature (Parnian et al., 2017). As an increase in the GO ratio, the reduction in WU of the SPEEK/GO membrane was induced due to the presence of strong covalent bonds among the carbon atoms in the GO layer that prevents more water to enter, which indirectly increased the membrane stability. The proton conductivity of a polymer electrolyte membrane (PEM) is one of the most important characteristics affecting the power output and produced voltage. The results reveal that the proton conductivity of the as-synthesized composite membranes shows higher compared to Nafion117, as shown Table 3. The highest proton conductivity observed for SPEEK/GO3 was 2.88 mS cm^{-1}. This may be attributed to a strong interaction between the functional groups of GO and the sulfonic acid groups in polymer that facilitates the proton transfer path in the membrane. The high amount of WU is also an effective factor in improving performance of SPEEK/GO membranes compared with that of bare SPEEK. Due to the incorporation of GO nanosheets into membranes, the higher proton conductivity was obtained for SPEEK/GO composite membranes compared to Nafion117, SPEEK15, and SPEEK20. It is important to state that the excess number of available ion exchange sites on the surface of GO and SPEEK

Table 3
IEC, WU, and DS amount of prepared membranes.

Membranes	IEC (meq g^{-1})	WU (%)	R_{int} (Ω)	σ (mS cm^{-1})	k_0 (cm s^{-1})	D_0 (cm^2 s^{-1})
Nafion117	1.00	44.31	3.63	2.20	9.5×10^{-4}	1.71×10^{-5}
SPEEK15	1.50	58.21	4.22	1.90	7.3×10^{-4}	1.27×10^{-5}
SPEEK20	1.30	55.00	8.01	1.00	6.4×10^{-4}	1.14×10^{-5}
SPEEK/GO1	1.57	67.85	3.59	2.23	5.0×10^{-4}	9.06×10^{-6}
SPEEK/GO3	2.21	62.72	2.78	2.88	4.8×10^{-4}	8.67×10^{-6}
SPEEK/GO5	1.93	61.23	3.14	2.55	4.1×10^{-4}	7.45×10^{-6}

accordingly increases the per cluster volume of ionic sites in SPEEK/GO matrix, which increases the proton conductivity of composite membranes. This is in agreement with the previous study (Vinothkannan et al., 2016). The proton conductivity value of the composite membrane tends to decrease with increasing GO content to 5% because the excess loading of GO nanosheets limits the polymer chain movement in the ionic cluster area and ionic transfer channels can be blocked, which cause the reduction of proton conductivity. The results of the study are in good consistent with the study on SGO incorporation into the bare SPEEK membranes where the loading contents over 7% cause a significant decrease in proton conductivity (Heo et al., 2013). Considering the results, at 3 wt% of GO loading, a SPEEK composite membrane is desirable for MFCs application.

As can be seen from Table 3, a significantly higher oxygen diffusion coefficient (D_o) and oxygen mass transfer coefficient (k_o) for the commercial Nafion 117 was obtained as $D_o = 1.71 \times 10^{-5}\ cm^2\ s^{-1}$ and $k_o = 9.5 \times 10^{-4}\ cm\ s^{-1}$, respectively, as one of its limitations. As listed in Table 3, GO incorporation resulted in a decrease in the oxygen diffusion coefficient and oxygen mass transfer coefficient through the membranes. The as-synthesized nanocomposite membranes demonstrated comparatively better results with oxygen diffusion coefficient and oxygen mass transfer coefficient over the bare SPEEK and the commercial Nafion 117. In addition, SPEEK/GO5 nanocomposite membrane showed the minimum oxygen diffusion coefficient and the oxygen mass transfer coefficient among the various GO fillers employed. The D_o values of SPEEK20 and SPEEK15 wt% were obtained to be 1.14×10^{-5} and $1.27 \times 10^{-5}\ cm^2\ s^{-1}$, respectively, when DI water was used as the catholyte. The results indicated that an increase in the GO content from 1 wt % to 5 wt% led to less oxygen diffusion. The oxygen diffusion coefficient and the oxygen mass transfer coefficient for the as-synthesized SPEEK/GO3 were estimated as $D_o = 8.67 \times 10^{-6}\ cm^2\ s^{-1}$ and $k_o = 4.8 \times 10^{-4}\ cm\ s^{-1}$, respectively, indicating that high content of GO nanosheets acted as a hindrance between hydrophilic channels and barrier pathway for both the physical and structural of oxygen diffusion. A higher oxygen diffusion coefficient is considered a disadvantage, shifting microbial metabolism to less efficient anaerobic respiration. On the other hand, limitation of anaerobic growth of microorganisms moves from anaerobic to aerobic conditions. The study confirms that GO can be incorporated within the PVA nanocomposite polymer matrix, which was reduced the limited free volume of the membrane matrix and was achieved the lower amount of oxygen diffusivity across the membrane (Rudra et al., 2017).

3.4. Performance of the MFC system

In the present study, the role of various types of PEMs on the performance of MFCs was evaluated according to produced power density. The industrial wastewater and anaerobic mixed bacteria sludge were used as anolyte in MFC systems. In batch mode operation, the polarization curves were obtained at steady-state conditions by setting an adjustable resistance in the data logger. The initial COD of all MFC systems was in the range of 1785-2190 mg l^{-1}.

Fig. 7 displays the polarization curve and voltage output of the MFCs assembled Nafion 117, SPEEK20, SPEEK15, SPEEK/GO1, SPEEK/GO3, and SPEEK/GO5 and. Table 4 summarizes the data for maximum power density, maximum current density, coulombic efficiency (CE), and COD removal of the aforementioned MFC assembled membranes. As shown in Fig. 7, the power density starts increasing and reaching a maximum value before it starts to fall down based on the proton conductivities of the membranes employed. Based on the results, a power density of 25.13 mW m^{-2} was generated with the MFC assembled commercial Nafion117. The corresponding CE of $2.17 \pm 0.12\%$ and COD removal efficiency of $81.91 \pm 0.32\%$ were obtained for the MFC assembled commercial Nafion117. In order to optimize the concentration of polymer in casting solution, SPEEK solution of 15 wt% (consisted of 15 g SPEEK and 85 g DMAc) and 20 wt% (consisted of 20 g SPEEK and 80 g DMAc) as bare membranes, after cast on the glass plates, were solidified by dry method. The results show that SPEEK15 showed power density and current density of 28.58 mW m^{-2} and 186 mA/m^2, respectively. The corresponding CE and COD removal efficiency were observed as $2.52 \pm 0.13\%$ and $84.69 \pm 0.48\%$, respectively, for SPEEK15. In comparison, an increase in the power density was about 13.7% for SPEEK15 compared with commercial Nafion 117 (Fig. 7). Nevertheless, the power density and current density for the MFC assembled SPEEK20 were achieved as 22.27 mW m^{-2} and 173 mA/m^2, respectively (Table 4). The decrease in power density for SPEEK20 was 13% compared with commercial Nafion 117. The corresponding CE and COD removal efficiency were achieved as $2.20 \pm 0.13\%$ and $82.91 \pm 0.44\%$, respectively, for SPEEK20. Our results show that the maximum power density of 53.12 mW m^{-2} was generated with the MFC assembled SPEEK/GO3 (Fig. 7). In comparison, about two-fold increase in power density was observed for SPEEK/GO3 over the commercial Nafion 117. Correspondingly, the highest CE for the MFC assembled SPEEK/GO3 was obtained. As presented in Table 4, the CE of $3.74 \pm 0.18\%$ and COD removal efficiency of 88.71 ± 0.51 were obtained with the MFC assembled SPEEK/GO3. However, the CE values for SPEEK/GO1 and SPEEK/GO5 were obtained as 2.15 ± 0.16 and $2.71 \pm 0.13\%$, respectively. In addition, we achieved COD removal efficiencies of 84.55 ± 0.50 and $88.73 \pm 0.51\%$ with MFC assembled SPEEK/GO1 and SPEEK/GO5, respectively. Compared with commercial Nafion 117, the increase in power density for SPEEK/GO1 and SPEEK/GO3 was higher as shown in Fig. 7. These results indicate that SPEEK solution of 15 wt% and GO nanosheets of 3 wt% (consisted of 15 g SPEEK, 3 g GO and 82 g DMAc) can be the best for the fabrication of nanocomposite membranes. Generally, membranes with higher proton conductivity would have a lower internal resistance which would yield higher power density (Ghasemi et al., 2013). Except for the SPEEK20, the power density of

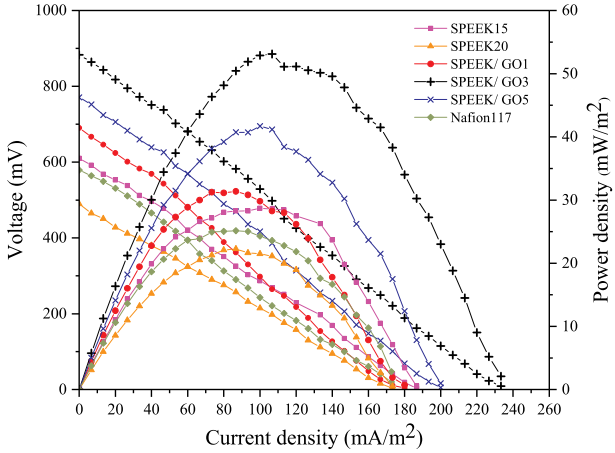

Fig. 7. Polarization curves of membranes applied in MFCs.

Table 4
Coulombic efficiency and COD removal of composite membranes.

Membranes	Max. current density (mA/m^2)	Max. power density (mW m^{-2})	Coulombic efficiency (%)	COD removal (%)
Nafion117	172.67	25.13	2.17 ± 0.12	81.91 ± 0.32
SPEEK15	186	28.70	2.52 ± 0.13	84.69 ± 0.48
SPEEK20	173	22.27	2.20 ± 0.11	82.91 ± 0.44
SPEEK/GO1	180	31.37	2.15 ± 0.16	84.55 ± 0.50
SPEEK/GO3	240.00	53.12	3.74 ± 0.18	88.71 ± 0.29
SPEEK/GO5	200	41.70	2.71 ± 0.13	88.73 ± 0.51

MFC assembled Nafion117 was less compared with all the other as-synthesized membranes which significant differences were observed. In a related study, the SPEEK electrolyte membrane was compared with the commercial Nafion 117 in a single chamber MFC system using *Escherichia coli*, which obtained comparatively a better performance in power density over the Nafion 117 (Ayyaru and Dharmalingam, 2011). In addition, the open-circuit voltage (OCV) values for SPEEK/GO3, SPEEK/GO5, SPEEK/GO1, SPEEK15, Nafion117, and SPEEK20 were obtained as 883, 771, 690, 610, 579, 490 mV, respectively. As a comparison, various membranes were tested as electrolyte in the MFC system, the COD removal efficiency levels of all systems were the same, but resulting in different levels of produced power density and CE. This could be due to the dependence of the power generation on the proton conductivity and oxygen diffusivity of the as-synthesized membranes, which might enhance the internal resistance, leading to a lower current density and power density (Fan et al., 2007). In a previous study, a CE of 4.09% was reported for the bio-electro-Fenton MFC assembled commercial Nafion117 (Birjandi et al., 2016). The higher CE may be due to the higher flow of current across the external circuit.

Summing up, a decrease in cell voltage was observed with an increase of SPEEK concentration in casting solution from 15 to 20 wt%, which is due to an increase of internal resistance of the membranes. In terms of power density, there was no significant difference between commercial Nafion117 membrane and the bare SPEEK20 membranes, but SPEEK15 showed higher cell voltage than Nafion117. Furthermore, the incorporation of GO nanosheets has improved the efficiency of MFC in terms of power produced due to its occupation into the free volume of the SPEEK matrix. The hydrophilic sites of the GO in the oxygenated functional groups (hydroxyl, carboxylic acid and epoxide groups) attached to the sp^3 carbon surface attracted the protons, which move through the hydrogen-bonding networks along the film of water molecules and transferred them by the Grotthuss mechanism through the formation or cleavage of covalent bonds (Karim et al., 2013). In addition, an increase of GO content in the casting solution from 1 to 3 wt% caused a significant increase in power density and coulombic efficiency values while further increase in GO nanosheets up to 5% resulted in a decrease in MFC efficiency. Our finding in agreement with the earlier research, which highlighted the novelty of incorporation of GO filled sulfonated polystyrene (SS)/polyvinyl alcohol (PVA) membrane in MFC application (Rudra et al., 2017).

3.5. Comparison of the studies

The choice of suitable membranes separating anode and cathode chamber is vital since it plays an important role in preventing the sludge and substrate entering the cathode and blocking the oxygen diffusion from the cathode to anode. However, poor separators could eventually lower the power output of the MFC and reduce COD removal efficiency in MFC.

Table 5 exhibits different parameters of several studies with MFCs, which used commercial Nafion, SPEEK, and composite membranes as PEMs. In the present study, COD removal was also monitored to control the treatment efficiency and energy generation from the wastewater. As shown in Table 5, no studies have focused on investigating the effects of different ratios of GO nanosheets on the efficiency of the membranes applied in MFCs. Leong et al. (2015) have published interesting research on sulfonated polymer based on the SPEEK/GO electrolyte nanocomposite membrane for their application in the MFC system. Unfortunately, their work has only focused on the fabrication of electrolyte composite membrane consisted of 15 wt% SPEEK and 0.25 wt% GO as casting solution (Leong et al., 2015). They have reported that the MFC with SPEEK/GO electrolyte membrane gave a peak power density of 900 mW m^{-2} and coulombic efficiency of 16.88% at a current density of 2.11 A m^{-2}, whereas the WU and COD removal efficiency were obtained as 83.01% and 85.4%, respectively. Meanwhile, inorganic nanoparticles were incorporated with the synthesized composite membranes, which resulted in the improved proton conductivity and hydrophobicity of the surfaces. Venkatesan and Dharmalingam (2015) developed a SPEEK-rutile TiO_2 electrolyte membrane with better performance of power density and IEC compared with bare SPEEK membrane. Furthermore, another study reported that the loading content of sulfonated SiO_2 improved effectively the proton conductivity of the SPEEK membrane and showed the highest maximum power density compared with SPEEK and SPEEK-SiO_2 in a single-chambered MFC (Sivasankaran

Table 5
Performance comparison of MFCs with various CEM membranes in power generation, COD removal, coulombic efficiency, ion exchange capacity, and water uptakehttps://www.sciencedirect.com/topics/social-sciences/energy-conversion.

CEM	Thickness (μm)	WU (%)	IEC (meq g^{-1})	COD removal (%)	Power density (mW m^{-2})	Refs.
SPEEK	180.0	15.85	1.47	n.d.	77.00	Venkatesan and Dharmalingam (2015)
SPEEK/TiO_2 7.5 wt%	180.0	21.83	1.98	n.d	98.10	
Nafion 117	190.0	22.00	1.23		47.50	
SPEEK/SiO_2 7.5 wt%	120.0	39.00	1.80	n.d	1008.0	Sivasankaran and Sangeetha (2015)
SPEEK	200.0	15.87	1.87	80.00	670.00	Ayyaru and Dharmalingam (2011)
SPEEK	170.0	27.00	1.23	–	–	Ayyaru and Dharmalingam (2014)
GO/SPEEK	–	85.40	–	83.01	902.00	Leong et al. (2015)
PES/SPEEK 5 wt%	150.0	–	–	68.00	170.00	Lim et al. (2012)
PS/SPEEK (29 wt%)	–	22.00	–	86.00	97.47	Ghasemi et al. (2016)
PS/SPEEK (76 wt%)	–	37.00	–	99.00	41.42	
Nafion 112	50.8	28.00	1.10	98.00	19.70	Ilbeygi et al. (2015)
Nafion 112	50.8	33.00	0.80	90.00	13.99	Ghasemi et al. (2012)
Nafion 117	175.0	–	0.98	63.50	68.90	Samsudeen et al. (2015)
Nafion 117	180.0	44.31	1.00	81.91	25.13	Present study
SPEEK15	180.0	58.21	1.50	84.69	28.58	
SPEEK20	180.0	55.00	1.30	82.91	22.27	
SPEEK/GO1	180.0	67.85	1.57	84.55	31.37	
SPEEK/GO3	180.0	62.72	2.21	88.71	53.12	
SPEEK/GO5	180.0	61.23	1.93	88.73	41.17	

and Sangeetha, 2015). In this regard, the power density and IEC of the combination materials were obtained up to 1008 mW m^{-2} and 1.8 meq g^{-1} for the composite membrane containing 7.5 wt% SiO_2– SO_3H. The researches have tended to focus on blending different types of polymers in order to achieve higher electrochemical performance. Lim et al. (2012) studied a combination of SPEEK/polyethersulfone (PES) membranes in the MFC system. Their results showed that the power density of 170 mW m^{-2} and COD removal efficiency of 68% were achieved for the composite membrane containing 5 wt% of SPEEK added into PES membrane. Ghasemi et al. (2016) studied electrochemical properties and MFC performance of PS/SPEEK composite membranes with two different sulfonation degree (DS). The results showed an increase in COD removal efficiency with increasing DS, while power density decreased with increasing the level of DS, but has lower power density compared to PES/SPEEK reported earlier. Additionally, some authors have reported studies in application of Nafion membranes in MFCs. The MFC with the Nafion 117 membrane showed reasonably higher peak power density if compared to that of cells with Nafion 112 membranes. In the present study, the peak power density of 25.13 mWm^{-2} for Nafion 117 was achieved. It should be taken into account that the bioelectrochemical systems owed different characteristics such as working volume, membrane surface, electrode area, membrane thickness, initial COD, and mixed liquor suspended solids. Thus, based on the information provided in Table 5, it is not possible to judge the performance of MFCs, but enough to follow the positive effects of incorporation of nanosheets and their ability as a good alternative to Nafion.

Based on the results reported in the literature, there are significant differences between systems in terms of power density, but overall COD removal of all the MFC systems assembled SPEEK/GO membranes was slightly better than that of commercial Nafion membrane. This indicated the equal ability of various MFCs in terms of anaerobic wastewater treatment. As shown in Table 5, the high COD removal efficiencies were obtained for SPEEK/GO5 and SPEEK/GO3. To sum up, the developed GO composite membranes reported here exhibit high power density and high coulombic efficiency compared to commercial Nafion. In addition to this, it seems that GO is potentially interesting to be used as an electrolyte membrane in the MFC system.

4. Conclusion

In the present study, the incorporation of nanosize GO to SPEEK membrane composite was conducted to investigate the effect of bending ratio on MFC efficiency in terms of power produced and COD removal. The results revealed that the membrane with 3% GO in SPEEK (SPEEK/GO3) showed the best results followed by SPEEK/GO5 and SPEEK/GO1, which indicates the positive effect of nanosheets blending on membrane properties and efficiency. Compared with the commercial membrane (Nafion117), the SPEEK/GO membrane showed to have greater advantages in the water uptake (WU), power density, voltage, coulombic efficiency (CE) and chemical oxygen demand (COD) removal. All the synthesized membranes were higher in efficiency comparing to Nafion117 except SPEEK20 which lower efficiency could be resulted by membrane internal resistance. In terms of COD removal, all membranes showed relatively equal but slightly higher for SPEEK/GO3 as for CE the best of 3.74% was obtained for the same membrane because of its role in power produced, maximum current and COD changes. The evidence from this study suggests that the blended SPEEK/GO composite membrane could be an encouraging candidate to replace the expensive perfluorosulfonic acid membrane Nafion as a separator in the MFC system. Furthermore, the incorporation of various nanoparticles into the sulfonated polymer electrolyte may improve the electrochemical characteristics and the combination of electricity generation and organic carbon, nitrogen and phosphorus removal from waste streams.

Acknowledgment

This study was supported by the Iran National Science Foundation (Grant No. 97014305). The authors wish to acknowledge the Environmental nanobiotechnology lab, Tarbiat Modares University, Noor, Iran for the facilities provided to accomplish the present research.

Appendix A. Supplementary data

Supplementary data to this article can be found online at https://doi.org/10.1016/j.bcab.2019.101369.

References

Alazmi, A., Rasul, S., Patole, S.P., Costa, P.M.F.J., 2016. Comparative study of synthesis and reduction methods for graphene oxide. Polyhedron 116, 153–161. https://doi.org/10.1016/j.poly.2016.04.044.

Amiri, A., Shanbedi, M., Ahmadi, G., Eshghi, H., Kazi, S.N., Chew, B.T., Savari, M., Zubir, M.N.M., 2016. Mass production of highly-porous graphene for high-performance supercapacitors. Sci. Rep. 6, 32686. https://doi.org/10.1038/srep32686.

Angioni, S., Millia, L., Bruni, G., Tealdi, C., Mustarelli, P., Quartarone, E., 2016. Improving the performances of Nafion™-based membranes for microbial fuel cells with silica-based, organically-functionalized mesostructured fillers. J. Power Sources 334, 120–127. https://doi.org/10.1016/j.jpowsour.2016.10.014.

Ayyaru, S., Dharmalingam, S., 2014. Enhanced response of microbial fuel cell using sulfonated poly ether ether ketone membrane as a biochemical oxygen demand sensor. Anal. Chim. Acta 818, 15–22. https://doi.org/10.1016/j.aca.2014.01.059.

Ayyaru, S., Dharmalingam, S., 2011. Development of MFC using sulphonated polyether ether ketone (SPEEK) membrane for electricity generation from waste water. Bioresour. Technol. 102, 11167–11171. https://doi.org/10.1016/j.biortech.2011.09.021.

Bakonyi, P., Koók, L., Kumar, G., Tóth, G., Rózsenberszki, T., Nguyen, D.D., Chang, S.W., Zhen, G., Bélafi-Bakó, K., Nemestóthy, N., 2018. Architectural engineering of bioelectrochemical systems from the perspective of polymeric membrane separators: a comprehensive update on recent progress and future prospects. J. Membr. Sci. 564, 508–522. https://doi.org/10.1016/j.memsci.2018.07.051.

Bhawal, P., Ganguly, S., Chaki, T.K., Das, N.C., 2016. Synthesis and characterization of graphene oxide filled ethylene methyl acrylate hybrid nanocomposites. RSC Adv. 6, 20781–20790. https://doi.org/10.1039/C5RA24914G.

Birjandi, N., Younesi, H., Ghoreyshi, A.A., Rahimnejad, M., 2016. Electricity generation through degradation of organic matters in medicinal herbs wastewater using bio-electro-Fenton system. J. Environ. Manag. 180, 390–400. https://doi.org/10.1016/j.jenvman.2016.05.073.

Bunlengsuwan, P., Paradee, N., Sirivat, A., 2017. Influence of sulfonated graphene oxide on sulfonated polysulfone membrane for direct methanol fuel cell. Polym. Plast. Technol. Eng. 56, 1695–1703. https://doi.org/10.1080/03602559.2017.1289398.

Bykkam, S., Rao, V., Chakra, S., Thunugunta, T., 2013. Synthesis and characterization of graphene oxide and its antimicrobial activity against Klebseilla and Staphylococus. Int. J. Adv. Biotechnol. Res. 4, 142–146.

Cao, N., Zhou, C., Wang, Y., Ju, H., Tan, D., Li, J., 2018. Synthesis and characterization of sulfonated graphene oxide reinforced sulfonated poly (ether ether ketone) (SPEEK) composites for proton exchange membrane materials. Materials (Basel) 11, 516. https://doi.org/10.3390/ma11040516.

Chae, K.J., Choi, M., Ajayi, F.F., Park, W., Chang, I.S., Kim, I.S., 2008. Mass transport through a proton exchange membrane (Nafion) in microbial fuel cells †. Energy Fuels 22, 169–176. https://doi.org/10.1021/ef700308u.

Chae, K.J., Kim, K.Y., Choi, M.J., Yang, E., Kim, I.S., Ren, X., Lee, M., 2014. Sulfonated polyether ether ketone (SPEEK)-based composite proton exchange membrane reinforced with nanofibers for microbial electrolysis cells. Chem. Eng. J. 254, 393–398. https://doi.org/10.1016/j.cej.2014.05.145.

Changkhamchom, S., Sirivat, A., 2010. Synthesis and properties of sulfonated poly(ether ketone ether sulfone) (S-PEKES) via bisphenol S: effect of sulfonation. Polym. Bull. 65, 265–281. https://doi.org/10.1007/s00289-010-0243-8.

Dai, W., Shen, Y., Li, Z., Yu, L., Qiu, X., 2014. Membranes with superior cyclability for highly efficient vanadium redox flow battery. J. Mater. Chem. A 2, 12423–12432. https://doi.org/10.1039/c4ta02124j.

Daud, W.R.W., Ghasemi, M., Chong, P.S., Jahim, J.M., Lim, S.S., Ismail, M., 2011. SPEEK/PES composite membranes as an alternative for proton exchange membrane in microbial fuel cell (MFC). In: 2011 IEEE 1st Conference on Clean Energy and Technology, CET 2011. IEEE, pp. 400–403. https://doi.org/10.1109/CET.2011.6041505.

Dimiev, A.M., Tour, J.M., 2014. Mechanism of graphene oxide formation. ACS Nano 8, 3060–3068. https://doi.org/10.1021/nn500606a.

Duan, Q., Ge, S., Wang, C., 2013. Water uptake , ionic conductivity and swelling properties of anion-exchange membrane. J. Power Sources 243, 773–778. https://doi.org/10.1016/j.jpowsour.2013.06.095.

Eck, M., Krueger, M., 2013. Thiol Functionalized Reduced Graphene Oxide as a Base Material for Novel Graphene- Nanoparticle Hybrid Composites, vol 231, pp. 146–154. https://doi.org/10.1016/j.cej.2013.07.007.

Fan, Y., Hu, H., Liu, H., 2007. Enhanced Coulombic efficiency and power density of air-cathode microbial fuel cells with an improved cell configuration. J. Power Sources 171, 348–354. https://doi.org/10.1016/j.jpowsour.2007.06.220.
Feng, J., Guo, Z., 2019. Wettability of graphene: from influencing factors and reversible conversions to potential applications. Nanoscale Horiz 4, 339–364. https://doi.org/10.1039/C8NH00348C.
Fischer, S.A., Dunlap, B.I., Gunlycke, D., 2018. Correlated dynamics in aqueous proton diffusion. Chem. Sci. 9, 7126–7132. https://doi.org/10.1039/C8SC01253A.
Genovese, A., Villante, C., 2014. Environmental analysis of hydrogen-methane blends for transportation. In: Membranes for Clean and Renewable Power Applications. Elsevier, pp. 218–234. https://doi.org/10.1533/9780857098658.3.218.
Ghasemi, M., Daud, W.R.W., Ismail, A.F., Jafari, Y., Ismail, M., Mayahi, A., Othman, J., 2013. Simultaneous wastewater treatment and electricity generation by microbial fuel cell: performance comparison and cost investigation of using Nafion 117 and SPEEK as separators. Desalination 325, 1–6. https://doi.org/10.1016/j.desal.2013.06.013.
Ghasemi, M., Shahgaldi, S., Ismail, M., Yaakob, Z., Daud, W.R.W., 2012. New generation of carbon nanocomposite proton exchange membranes in microbial fuel cell systems. Chem. Eng. J. 184, 82–89. https://doi.org/10.1016/j.cej.2012.01.001.
Ghasemi, M., Wan Daud, W.R., Alam, J., Ilbeygi, H., Sedighi, M., Ismail, A.F., Yazdi, M. H., Aljlil, S.A., 2016. Treatment of two different water resources in desalination and microbial fuel cell processes by poly sulfone/Sulfonated poly ether ether ketone hybrid membrane. Energy 96, 303–313. https://doi.org/10.1016/j.energy.2015.12.053.
Hayyan, M., Abo-Hamad, A., AlSaadi, M.A., Hashim, M.A., 2015. Functionalization of graphene using deep eutectic solvents. Nanoscale Res. Lett. 10, 1004. https://doi.org/10.1186/s11671-015-1004-2.
Heilmann, J., Logan, B.E., 2006. Production of electricity from proteins using a microbial fuel cell. Water Environ. Res. 78, 531–537. https://doi.org/10.2175/106143005X73046.
Heo, Y., Im, H., Kim, J., 2013. The effect of sulfonated graphene oxide on Sulfonated Poly (Ether Ether Ketone) membrane for direct methanol fuel cells. J. Membr. Sci. 425–426, 11–22. https://doi.org/10.1016/j.memsci.2012.09.019.
Hernández-Flores, G., Poggi-Varaldo, H.M., Solorza-Feria, O., 2016. Comparison of alternative membranes to replace high cost Nafion ones in microbial fuel cells. Int. J. Hydrogen Energy 1, 2–10. https://doi.org/10.1016/j.ijhydene.2016.08.206.
Hummers, W.S., Offeman, R.E., 1958. Preparation of graphitic oxide. J. Am. Chem. Soc. 80, 1339–1339. https://doi.org/10.1021/ja01539a017.
Hwang, K., Kim, J.H., Kim, S.Y., Byun, H., 2014. Preparation of polybenzimidazole-based membranes and their potential applications in the fuel cell system. Energies 7, 1721–1732. https://doi.org/10.3390/en7031721.
Ilbeygi, H., Ghasemi, M., Emadzadeh, D., Ismail, A.F., Zaidi, S.M.J., Aljlil, S.A., Jaafar, J., Martin, D., Keshani, S., 2015. Power generation and wastewater treatment using a novel SPEEK nanocomposite membrane in a dual chamber microbial fuel cell. Int. J. Hydrogen Energy 40, 477–487. https://doi.org/10.1016/j.ijhydene.2014.10.026.
Kamaroddin, M.F.A., Sabli, N., Abdullah, T.A.T., Abdullah, L.C., Izhar, S., Ripin, A., Ahmad, A., 2019. Phosphoric acid doped polybenzimidazole and sulfonated polyether ether ketone composite membrane for hydrogen production in high-temperature copper chloride electrolysis. In: IOP Conference Series: Earth and Environmental Science. IOP Publishing, p. 12057.
Karim, M.R., Hatakeyama, K., Matsui, T., Takehira, H., Taniguchi, T., Koinuma, M., Matsumoto, Y., Akutagawa, T., Nakamura, T., Noro, S., Yamada, T., Kitagawa, H., Hayami, S., 2013. Graphene oxide nanosheet with high proton coknductivity. J. Am. Chem. Soc. 135, 8097–8100. https://doi.org/10.1021/ja401060q.
Kim, J.R., Premier, G.C., Hawkes, F.R., Rodríguez, J., Dinsdale, R.M., Guwy, A.J., 2010. Modular tubular microbial fuel cells for energy recovery during sucrose wastewater treatment at low organic loading rate. Bioresour. Technol. 101, 1190–1198. https://doi.org/10.1016/j.biortech.2009.09.023.
Koók, L., Bakonyi, P., Harnisch, F., Kretzschmar, J., Chae, K.-J., Zhen, G., Kumar, G., Rózsenberszki, T., Tóth, G., Nemestóthy, N., Bélafi-Bakó, K., 2019. Biofouling of membranes in microbial electrochemical technologies: causes, characterization methods and mitigation strategies. Bioresour. Technol. 279, 327–338. https://doi.org/10.1016/j.biortech.2019.02.001.
Koók, L., Quéméner, E.D.-L., Bakonyi, P., Zitka, J., Trably, E., Tóth, G., Pavlovec, L., Pientka, Z., Bernet, N., Bélafi-Bakó, K., Nemestóthy, N., 2019. Behavior of two-chamber microbial electrochemical systems started-up with different ion-exchange membrane separators. Bioresour. Technol. 278, 279–286. https://doi.org/10.1016/j.biortech.2019.01.097.
Kumar, R., Mamlouk, M., Scott, K., 2014. Sulfonated polyether ether ketone – sulfonated graphene oxide composite membranes for polymer electrolyte fuel cells. RSC Adv. 4, 617–623. https://doi.org/10.1039/C3RA42390E.
Kumar, S.S., Bishnoi, N.R., 2017. Coagulation of landfill leachate by FeCl 3 : process optimization using Box – Behnken design (RSM). Appl. Water Sci. 7, 1943–1953. https://doi.org/10.1007/s13201-015-0372-1.
Kumar, S.S., Kumar, V., Malyan, S.K., Sharma, J., Mathimani, T., Maskarenj, M.S., Ghosh, P.C., Pugazhendhi, A., 2019. Microbial fuel cells (MFCs) for bioelectrochemical treatment of different wastewater streams. Fuel 254, 115526. https://doi.org/10.1016/j.fuel.2019.05.109.
Lee, H.S., Parameswaran, P., Kato-Marcus, A., Torres, C.I., Rittmann, B.E., 2008. Evaluation of energy-conversion efficiencies in microbial fuel cells (MFCs) utilizing fermentable and non-fermentable substrates. Water Res. 42, 1501–1510. https://doi.org/10.1016/j.watres.2007.10.036.
Leong, J.X., Daud, W.R.W., Ghasemi, M., Ahmad, A., Ismail, M., Liew, K. Ben, 2015. Composite Membrane Containing Graphene Oxide in Sulfonated Polyether Ether Ketone in Microbial Fuel Cell Applications, International Journal of Hydrogen Energy. Elsevier Ltd. https://doi.org/10.1016/j.ijhydene.2015.04.082.
Lim, S.S., Daud, W.R.W., Md Jahim, J., Ghasemi, M., Chong, P.S., Ismail, M., 2012. Sulfonated poly(ether ether ketone)/poly(ether sulfone) composite membranes as an alternative proton exchange membrane in microbial fuel cells. Int. J. Hydrogen Energy 37, 11409–11424. https://doi.org/10.1016/j.ijhydene.2012.04.155.
Lin, H., Dangwal, S., Liu, R., Kim, S., Li, Y., Zhu, J., 2018. Reduced wrinkling in GO membrane by grafting basal-plane groups for improved gas and liquid separations. J. Membr. Sci. 563, 336–344. https://doi.org/10.1016/j.memsci.2018.05.073.
Logan, B.E., Verstraete, W., 2017. Microbial Fuel Cells : Methodology and Technology † Critical Review Microbial Fuel Cells : Methodology and Technology †. https://doi.org/10.1021/es0605016.
Lv, Z., Chen, Y., Wei, H., Li, F., Hu, Y., Wei, C., Feng, C., 2013. One-step electrosynthesis of polypyrrole/graphene oxide composites for microbial fuel cell application. Electrochim. Acta 111, 366–373. https://doi.org/10.1016/j.electacta.2013.08.022.
Mamlouk, M., Scott, K.Ã., 2011. Phosphoric Acid-Doped Electrodes for a PBI Polymer Membrane Fuel Cell, pp. 507–519. https://doi.org/10.1002/er.
Marcano, D.C., Kosynkin, D.V., Berlin, J.M., Sinitskii, A., Sun, Z., Slesarev, A., Alemany, L.B., Lu, W., Tour, J.M., 2010. Improved synthesis of graphene oxide. ACS Nano 4, 4806–4814. https://doi.org/10.1021/nn1006368.
Mauritz, K.A., Moore, R.B., 2004. State of understanding of Nafion. Chem. Rev. 104, 4535–4586. https://doi.org/10.1021/cr0207123.
Othman, M.H.D., Ismail, A.F., Mustafa, A., 2007. Physico-chemical study of sulfonated poly (ether ether ketone) membranes for direct. Methanol Fuel Cell Appl. 2, 10–28.
Parnian, M.J., Gashoul, F., Rowshanzamir, S., 2017. Studies on the SPEEK membrane with low degree of sulfonation as a stable proton exchange membrane for fuel cell applications. Iran J. Hydrog. Fuel Cell 3, 221–232.
Perumbilavil, S., Sankar, P., Priya Rose, T., Philip, R., 2015. White light Z-scan measurements of ultrafast optical nonlinearity in reduced graphene oxide nanosheets in the 400-700 nm region. Appl. Phys. Lett. 107. https://doi.org/10.1063/1.4928124.
Pupkevich, V., Glibin, V., Karamanev, D., 2007. The effect of ferric ions on the conductivity of various types of polymer cation exchange membranes. J. Solid State Electrochem. 11, 1429–1434. https://doi.org/10.1007/s10008-007-0306-4.
Rabaey, K., Clauwaert, P., Aelterman, P., Verstraete, W., 2005. Tubular microbial fuel cells for efficient electricity generation. Environ. Sci. Technol. 39, 8077–8082. https://doi.org/10.1021/es050986i.
Rahimnejad, M., Asghary, M., Fallah, M., 2020. Microbial fuel cell (MFC): an innovative technology for wastewater treatment and power generation. In: Bharagava, R.N., Saxena, G. (Eds.), Bioremediation of Industrial Waste for Environmental Safety. Springer Singapore, Singapore, pp. 215–235. https://doi.org/10.1007/978-981-13-3426-9_9.
Rahimnejad, M., Ghasemi, M., Najafpour, G.D.D., Ismail, M., Mohammad, A.W.W., Ghoreyshi, A.A., Hassan, S.H.A., 2012. Electrochimica Acta Synthesis , characterization and application studies of self-made Fe 3 O 4/PES nanocomposite membranes in microbial fuel cell. Electrochim. Acta 85, 700–706. https://doi.org/10.1016/j.electacta.2011.08.036.
Rattana, T., Chaiyakun, S., Witit-anun, N., Nuntawong, N., Chindaudom, P., 2012. Preparation and characterization of graphene oxide nanosheets. Procedia Eng 32, 759–764. https://doi.org/10.1016/j.proeng.2012.02.009.
Reyes-Rodriguez, J.L., Escorihuela, J., García-Bernabé, A., Giménez, E., Solorza-Feria, O., Compañ, V., 2017. Proton conducting electrospun sulfonated polyether ether ketone graphene oxide composite membranes. RSC Adv. 7, 53481–53491. https://doi.org/10.1039/C7RA10484G.
Rudra, R., Kumar, V., Pramanik, N., Kundu, P.P., Paban, P., 2017. Graphite oxide incorporated crosslinked polyvinyl alcohol and sulfonated styrene nanocomposite membrane as separating barrier in single chambered microbial fuel cell. J. Power Sources 341, 285–293. https://doi.org/10.1016/j.jpowsour.2016.12.028.
Samsudeen, N., Radhakrishnan, T.K., Matheswaran, M., 2015. Bioelectricity production from microbial fuel cell using mixed bacterial culture isolated from distillery wastewater. Bioresour. Technol. 195, 242–247. https://doi.org/10.1016/j.biortech.2015.07.023.
Seetharaman, S., Ramya, K., Dhathathreyan, K.S., 2013. Electrochemically reduced graphene oxide/sulfonated polyether ether ketone composite membrane for electrochemical applications. In: AIP Conference Proceedings, pp. 257–261. https://doi.org/10.1063/1.4810069.
Seo, S.-J., Kim, B.-C., Sung, K.-W., Shim, J., Jeon, J.-D., Shin, K.-H., Shin, S.-H., Yun, S.-H., Lee, J.-Y., Moon, S.-H., 2013. Electrochemical properties of pore-filled anion exchange membranes and their ionic transport phenomena for vanadium redox flow battery applications. J. Membr. Sci. 428, 17–23. https://doi.org/10.1016/j.memsci.2012.11.027.
Sivasankaran, A., Sangeetha, D., 2015. Influence of sulfonated SiO2 in sulfonated polyether ether ketone nanocomposite membrane in microbial fuel cell. Fuel 159, 689–696. https://doi.org/10.1016/j.fuel.2015.07.002.
Sowmya, G., Prabhu, M.R., 2018. Fabrication of blend polymer electrolyte membrane with poly (amide imide)-sulfonated poly (ether ether ketone) for microbial fuel cell. Mater. Res. Express 6, 025519. https://doi.org/10.1088/2053-1591/aaf2b9.
Sun, J., Hu, Y., Bi, Z., Cao, Y., 2009. Improved performance of air-cathode single-chamber microbial fuel cell for wastewater treatment using microfiltration membranes and multiple sludge inoculation. J. Power Sources 187, 471–479. https://doi.org/10.1016/j.jpowsour.2008.11.022.
Tiwari, B.R., Noori, M.T.T., Ghangrekar, M.M., 2016. A novel low cost polyvinyl alcohol-Nafion-borosilicate membrane separator for microbial fuel cell. Mater. Chem. Phys. 182, 86–93. https://doi.org/10.1016/j.matchemphys.2016.07.008.
Tommasi, T., Lombardelli, G., 2017. Energy sustainability of microbial fuel cell (MFC): a case study. J. Power Sources 356, 438–447. https://doi.org/10.1016/j.jpowsour.2017.03.122.

Venkatesan, P.N., Dharmalingam, S., 2015. Effect of cation transport of SPEEK – rutile TiO2 electrolyte on microbial fuel cell performance. J. Membr. Sci. 492, 518–527. https://doi.org/10.1016/j.memsci.2015.06.025.

Vinothkannan, M., Kannan, R., Kim, A.R., 2016. Facile Enhancement in Proton Conductivity of Sulfonated Poly (Ether Ether Ketone) Using Functionalized Graphene Oxide — Synthesis , Characterization , and Application towards Proton Exchange Membrane Fuel Cells 1197–1207. https://doi.org/10.1007/s00396-016-3877-8.

Wu, G., Lin, S.-J., Hsu, I.-C., Su, J.-Y., Chen, D.W., 2019. Study of high performance sulfonated polyether ether ketone composite electrolyte membranes. Polymers (Basel) 11, 1177. https://doi.org/10.3390/polym11071177.

Wu, N., She, X., Yang, D., Wu, X., Su, F., Chen, Y., 2012. Synthesis of network reduced graphene oxide in polystyrene matrix by a two-step reduction method for superior conductivity of the composite. J. Mater. Chem. 22, 17254–17261. https://doi.org/10.1039/C2JM33114D.

Xu, Q., Wang, L., Li, Chen, Wang, X., Li, Cuicui, Geng, Y., 2019. Study on improvement of the proton conductivity and anti-fouling of proton exchange membrane by doping SGO@SiO2 in microbial fuel cell applications. Int. J. Hydrogen Energy 44, 15322–15332. https://doi.org/10.1016/j.ijhydene.2019.03.238.

Yin, Y., Wang, H., Cao, L., Li, Zhen, Li, Zongyu, Gang, M., Wang, C., Wu, H., Jiang, Z., Zhang, P., 2016. Sulfonated poly(ether ether ketone)-based hybrid membranes containing graphene oxide with acid-base pairs for direct methanol fuel cells. Electrochim. Acta 203, 178–188. https://doi.org/10.1016/j.electacta.2016.04.040.

Zaidi, S.M.J., 2005. Preparation and characterization of composite membranes using blends of SPEEK/PBI with boron phosphate. Electrochim. Acta 50, 4771–4777. https://doi.org/10.1016/j.electacta.2005.02.027.

Zawodzinski, T.A., Derouin, C., Radzinski, S., Sherman, R.J., Smith, V.T., Springer, T.E., Gottesfeld, S., Soc, J.E., Zawodzinski, T.A., Derouin, C., Radzinski, S., Sherman, R.J., Smith, V.T., Springer, T.E., Gottesfeld, S., 1993. Membranes water uptake by and transport through nation | 117 membranes. J. Electrochem. Soc. 140, 1041–1047. https://doi.org/10.1149/1.2056194.

Zhang, Y., Liu, M., Zhou, M., Yang, H., Liang, L., Gu, T., 2019. Microbial fuel cell hybrid systems for wastewater treatment and bioenergy production: synergistic effects, mechanisms and challenges. Renew. Sustain. Energy Rev. 103, 13–29. https://doi.org/10.1016/J.RSER.2018.12.027.

Zhao, J., Guo, L., Wang, J., 2018. Synthesis of cation exchange membranes based on sulfonated polyether sulfone with different sulfonation degrees. J. Membr. Sci. 563, 957–968. https://doi.org/10.1016/j.memsci.2018.05.023.

Zhao, Z., 2018. Electrochemical properties of SPEEK/epoxy/graphene oxide composites as proton exchange membrane. Int. J. Electrochem. Sci. 13, 2945–2957. https://doi.org/10.20964/2018.03.03.

Zinadini, S., Zinatizadeh, A.A., Rahimi, M., Vatanpour, V., Rahimi, Z., 2017. High power generation and COD removal in a microbial fuel cell operated by a novel sulfonated PES/PES blend proton exchange membrane. Energy 125, 427–438. https://doi.org/10.1016/j.energy.2017.02.146.